ISSN 1392 – 1215 ELECTRONICS AND ELECTRICAL ENGINEERING 2010. No. 5(101)
ELEKTRONIKA IR ELEKTROTECHNIKA

T 190 ELECTRICAL ENGINEERING
ELEKTROS INŽINERIJA

# The Design of a Hall Effect Current Transformer and Examination of The Linearity with Real Time Parameter Estimation

**G. Gokmen, K. Tuncalp**
*Department of Electrical Education, Marmara University Technical Education Faculty*
*Goztepe Campus, 34722 Kadıkoy, Istanbul, Turkey, phone: +90 216 336 57 70 (265), e-mail: gokhang@marmara.edu.tr*

## Introduction

The Hall Effect Sensors have many application areas such as various protection circuits, analysis of magnetic field or current distribution. However, the most widespread application field of the Hall Effect sensors is the current sensing. If current sensing will be analog, linear Hall Effect sensors are preferred. The Hall sensor is placed to air gap of core for sensing magnetic flux. When current is passed through the conductor placed inside of the core, magnetic flux arises from current in the core and the Hall sensor generates a voltage proportional to the current. The linear response of sensed current is rather convenient for control feedback circuits [1, 2, 3, 4, 5].

The output voltage of sensor is same with the AC and DC wave shape of measured current. The air gap of the core isolates the sensor electrically and so, over current damage or high voltage transient on sensor is prevented. It also eliminates DC insertion loss [5].

The Hall Effect current transformer has a good linearity, however depending on structure of the Hall sensor, deviations may occur in offset voltages and defects resulting from environmental factors cause deterioration of linearity in current measurement. This study suggests more linear measurement by using a real time parameter estimation method.

## Hall Effect current measurement

The Hall sensor based current measurement can be realized as open loop or closed loop. While in open loop, there is no secondary winding, in closed loop, Hall voltage is transformed to current by means of a transistor circuit and passed from a secondary winding. The purpose is compensating of the magnetic flux created by primary winding. The basic connection scheme of such a current transformer is given in Fig. 1 [5].

The Hall sensor produces a voltage proportional to the magnetic flux and the primary current. The output voltage is amplified by an operational amplifier and applied to a push-pull transistor circuit so it is transformed to secondary current. In this way, a second magnetic flux is created to balance primary magnetic flux in the core. The secondary current is symmetric of the primary current and secondary winding is generally coiled as 1000 turns [5–7].

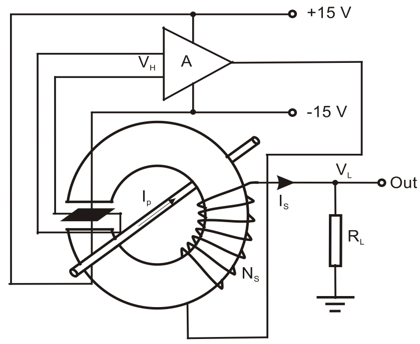


**Fig. 1.** Basic connection scheme of a closed loop current transformer

The basic equation is

$$N_p.I_p = N_s.I_s\,. \qquad (1)$$

The magnetic flux density in air gap must not be bigger than the maximum flux density that can be sensed by the sensor [8, 9]. The magnetic flux density is calculated with the following expression

$$B = \frac{4.\pi.10^{-7}.\mu_i.N_P.I_P}{l_m + l_g.\mu_i}\,, \qquad (2)$$

where $B$ – the magnetic flux density (T); $\mu_i$ – the initial permeability of the core; $N_P.I_P$ – the primary mmf; $l_m$ – the mean length of core (m); $l_g$ – the length of air gap (m). The effective permeability of core is calculated as flow [8–10]

$$\mu_e = \frac{B.l_m}{N_P.I_P}\,. \qquad (3)$$

## Design example and application results

In this study, Allegro A 3515 linear Hall sensor is preferred. The sensitivity of this sensor is $5 \times 10^4$ mV/T, the operating voltage is 5V. The operating magnetic flux range is ± 40 mT and ± 80 mT [11].

For $N_P.I_P = 30$ AT, $l_m = 54.2$ mm, $l_g = 1.8$ mm and $\mu_i = 3000$ values, the magnetic flux density is calculated as 0.0207 T. In this magnetic flux density, the output voltage of Hall sensor is 1.035 V. the effective permeability of core is calculated as $\mu_e = 3.738 \times 10^{-5}$ H/m. The connection scheme of the designed Hall Effect current transformer is given in Fig. 2 [12].

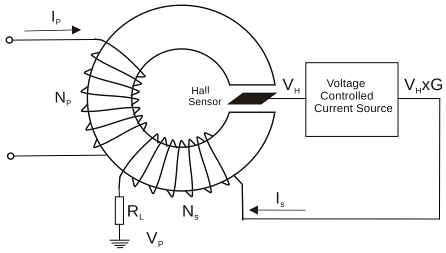


**Fig. 2.** The connection scheme of the designed Hall Effect current transformer

The voltage controlled current source is a circuit that purifies the Hall sensor output voltage from quiescent voltage output, amplifies and passes it through the secondary winding as current. (Fig. 3) [12]. The quiescent voltage output is generally half of the supply voltage ($V_{cc} / 2$) [9, 11]. The quiescent voltage output was made zero by adjusting the potentiometer in LM 741 subtraction circuit. (Fig. 3) [13, 14].

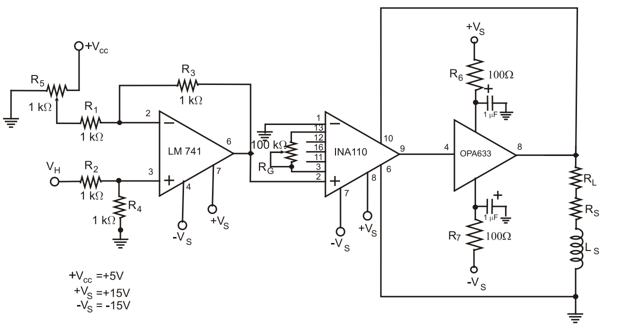


**Fig. 3.** Voltage controlled current source

For voltage amplification, INA 110 KP instrumentation amplifier by Texas Instruments Company was preferred [15]. The value of external gain resistor connected to input of the INA 110 KP is 81.58 kΩ for 1.49 voltage gain ratio (G) and is adjusted by 100 kΩ potentiometer (Fig. 3).

OPA 633 KP buffer was connected to output of the voltage amplification circuit to provide secondary current so a voltage controlled current source was obtained by driving the output of INA 110 KP with OPA 633 KP. [16, 17].

The secondary current is found with the following expression

$$I_S = \frac{V_H.G}{R_L + Z_S}, \qquad (4)$$

where $V_H$ indicates Hall sensor voltage, $R_L$ indicates measurement resistor, $Z_S$ indicates secondary winding impedance. The measurement voltage of the Hall Effect current transformer is

$$V_L = I_S \times R_L \; or \; V_L = \frac{V_H.G}{R_L + Z_S}.R_L . \qquad (5)$$

For the application, necessary air gap is established on the Magnetics OF-42206-TC ferrite core and primary and secondary windings are coiled. The core with Hall sensor and upper side view of the electronic circuit is given in Fig. 4 [13].

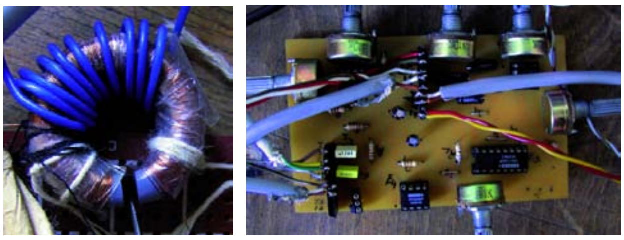

**Fig. 4.** The core with Hall Sensor and upper side view of the electronic circuit

Primary current of current transformer is increased by 0.05 A intervals and corresponding secondary currents and measurement voltages are measured as DC and AC (50 Hz, RMS) values, respectively. The environment temperature is 27.3 $^0$C. Transfer function of closed loop current transformer is given in Fig. 5. Nonlinearity clearly is shown especially 0-0.5 A area [12].

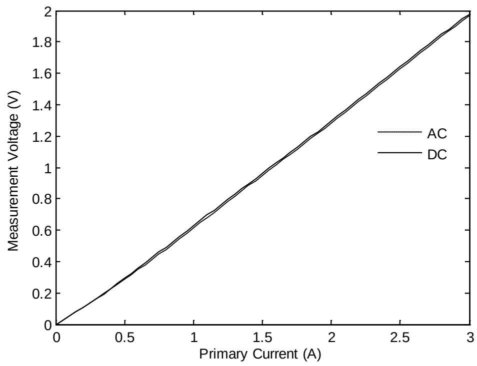


**Fig. 5.** Transfer function of closed loop current transformer

It is the current value that we aim to measure actual parameter and it requires converting measurement voltage to current value. We know existence of a constant ratio between measurement voltage ($V_L$) and primary current ($I_P$) [12]. This constant ratio ($C$) is 1.51723 (DC) and 1.52755 (AC) for maximum measurement voltage and primary current values. When we multiply $V_L$ by this constant ratio we can find out current ( $I_{P_c}$ ) which we aim to measure

$$I_{P_C} = C \times V_L \,. \tag{6}$$

**Examination of the linearity with real time parameter estimation**

If the equation of $N_p.I_p = N_s.I_s$ is provided completely, the primary mmf - secondary mmf changing curve is a regular increasing line. However, because of the various reasons given below, this curve can not be obtained completely:

a) Change in quiescent output voltage of linear Hall sensors depending on the earth magnetic effect, sensor supply voltage and temperature [9, 11, 12].

b) Change in sensitivity of Linear Hall sensors depending on sensor supply voltage and temperature [11].

c) The tolerance of the semiconductor elements used in voltage controlled current source. [14, 15, 17].

d) The linearity error depending on the selected core materials, air gap, core losses, DC magnetic offset (remanent magnetization of core material) [6].

e) Unbalance between the primary and secondary windings [18].

f) Random errors in the measurement system.

When Fig. 5 is examined, it is seen that $I_S = N_P.I_P / N_S$ condition can not be obtained exactly. This situation prevents us from carrying out accurate current measurement. For a more accurate calculation, mathematical expression of the transfer function of the current transformer should be examined. For this aim, equation parameters were found with real time parameter estimation. This method facilitates determination of physical parameters of the established model and making of calibration [19].

Let's find out expression of primary current depending on measurement voltage and let's express this current as estimated primary current ( $I_{P_E}$ ). If this expression is third degree polynomial, equation is

$${}_{P_E} = p_1.V_L^3 + p_2.V_L^2 + p_3.V_L \,. \tag{7}$$

To show the $n$ data number, sum of squares of the residuals S of the measured $I_{P_i}$ and estimated $I_{P_E}$ primary currents is [19, 20, 21]

$$S = \sum_{i=1}^{n}\left[ I_{Pi} - \left( p_1.V_L^3 + p_2.V_L^2 + p_3.V_L \right) \right]^2 , \tag{8}$$

where $p_1$, $p_2$ and $p_3$ parameters that will make this sum to be the least are calculated with expressions of

$$\frac{\partial S}{\partial p_1} = 0 = \sum_{i=1}^{n} 2\left[ I_{P_i} - \left( p_1.V_L^3 + p_2.V_L^2 + p_3.V_L \right) \right]\left( -V_L^3 \right), \tag{9}$$

$$\frac{\partial S}{\partial p_2} = 0 = \sum_{i=1}^{n} 2\left[ I_{P_i} - \left( p_1.V_L^3 + p_2.V_L^2 + p_3.V_L \right) \right]\left( -V_L^2 \right), \tag{10}$$

$$\frac{\partial S}{\partial p_3} = 0 = \sum_{i=1}^{n} 2\left[ I_{P_i} - \left( p_1.V_L^3 + p_2.V_L^2 + p_3.V_L \right) \right]\left( -V_L \right). \tag{11}$$

If necessary operations are made, the equations are written in matrix form and $p_1$, $p_2$ and $p_3$ parameters are left alone, Eq.(12) is obtained [19]

$$\begin{bmatrix} p_1 \\ p_2 \\ p_3 \end{bmatrix} = \begin{bmatrix} \sum_{i=1}^{n} V_{L_i}^6 & \sum_{i=1}^{n} V_{L_i}^5 & \sum_{i=1}^{n} V_{L_i}^4 \\ \sum_{i=1}^{n} V_{L_i}^5 & \sum_{i=1}^{n} V_{L_i}^4 & \sum_{i=1}^{n} V_{L_i}^3 \\ \sum_{i=1}^{n} V_{L_i}^4 & \sum_{i=1}^{n} V_{L_i}^3 & \sum_{i=1}^{n} V_{L_i}^2 \end{bmatrix}^{-1} \times \begin{bmatrix} \sum_{i=1}^{n} V_{L_i}^3 \times I_{P_i} \\ \sum_{i=1}^{n} V_{L_i}^2 \times I_{P_i} \\ \sum_{i=1}^{n} V_{L_i} \times I_{P_i} \end{bmatrix}. \tag{12}$$

All above calculations can be summarized as the parameter estimation process in Fig. 6 [22].

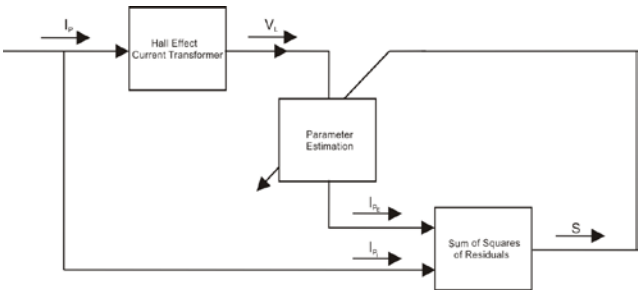


**Fig. 6.** The parameter estimation process

It requires reference primary current for real time simulation. The primary current is applied as ramp function. Input variable (primary current) and output variable (measurement voltage) were transferred to Matlab Simulink by PCI-1716 DAQ card. Graphical interface of simulation circuit is given in Fig. 7.

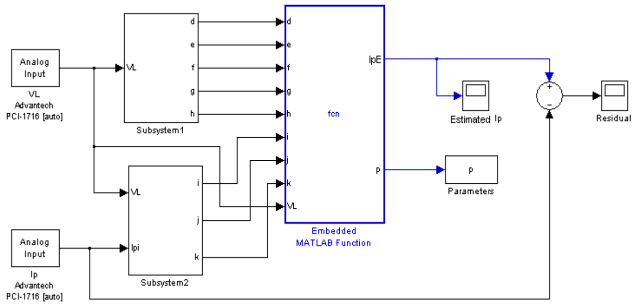


**Fig. 7.** Simulink circuit of real time parameter estimation

Matrix components in (12) were created in subsystem 1 and subsystem (Fig. 8). d, e, f, g, h denote $\sum_{i=1}^{n} V_{L_i}^2$, $\sum_{i=1}^{n} V_{L_i}^3$, $\sum_{i=1}^{n} V_{L_i}^4$, $\sum_{i=1}^{n} V_{L_i}^5$, $\sum_{i=1}^{n} V_{L_i}^6$ and i, j, k denote $\sum_{i=1}^{n} V_{L_i}^3.I_{P_i}$, $\sum_{i=1}^{n} V_{L_i}^2.I_{P_i}$, respectively.

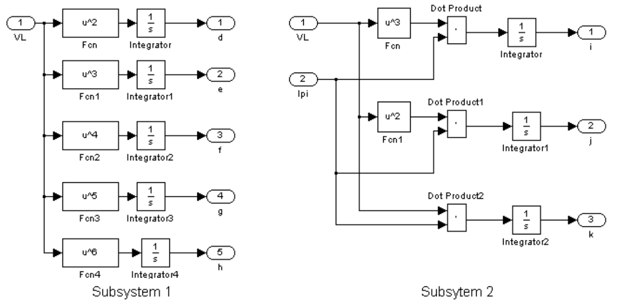


**Fig. 8.** Simulink circuits of subsystem 1 and subsystem 2

Embedded Matlab function block allow various Matlab functions to be used in simulink. Inputs of this block are d,e,f,g,h,i,j,k matrix components which are previously created by Subsystem1 and Subsytem2 and $V_L$. Outputs are parameter matrix $p$ ($p_1$, $p_2$, $p_3$) and real time estimated primary current value $I$ ($p_1.V_L^3 + p_2.V_L^2 + p_3.V_L$). Matlab command window in Embedded Matlab function block is given below:

```
function [IpE,p]= fcn(d,e,f,g,h,i,j,k,VL),
% Coefficients Matrix,
m=[h,g,f;g,f,e;f,e,d],
n=inv(m),
o=[i;j;k],
% Parameters,
p=n*o,
r=transpose (p),
t=[VL^3;VL^2;VL],
IpE =r*t.
```

Parameter matrix from (12) is

$$\begin{bmatrix} p_1 \\ p_2 \\ p_3 \end{bmatrix} = \begin{bmatrix} h & g & f \\ g & f & e \\ f & e & d \end{bmatrix}^{-1} \times \begin{bmatrix} i \\ j \\ k \end{bmatrix} \qquad (13)$$

and estimated primary current value at end of the parameter estimation is

$$IpE = \begin{bmatrix} p_1 & p_2 & p_3 \end{bmatrix} \times \begin{bmatrix} V_L^3 \\ V_L^2 \\ V_L \end{bmatrix}. \qquad (14)$$

Estimated primary current and residual for DC an AC measurements are given in Fig. 9 and 10.

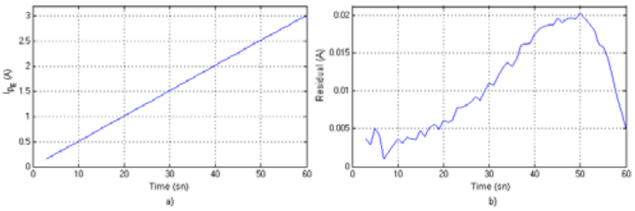


**Fig. 9.** DC simulation result: a – estimated primary current; b – residual

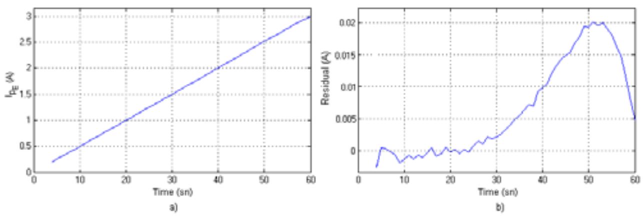


**Fig. 10.** AC simulation result: a – estimated primary current; b – residual

Because of the dimension of the parameter square matrix estimated primary current can be obtained after 3 seconds. Transfer function can be rearranged after parameter estimation resulting a much more accurate transfer function (Fig. 11).

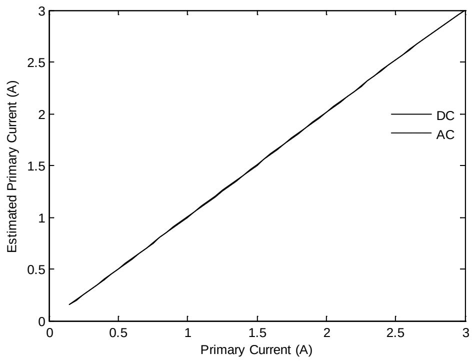


**Fig. 11.** New transfer function of Hall effect current transformer

Fig. 12 a) shows errors between reference primary current and calculated primary current depending on $V_L$ measurement voltage, Fig. 12 b) shows errors between reference primary current and estimated primary current

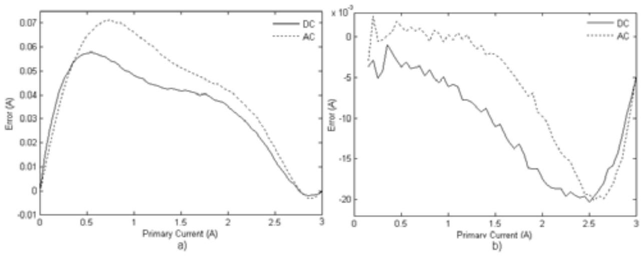


**Fig. 12.** Errors in measurements. a) Before estimation b) After estimation

Obtained parameters and estimated primary current values are shown in Table 1.

It is seen that AC error is bigger than DC error in both before and after estimation procedure because AC primary current naturally induces an error current in secondary winding. This phenomenon is operating principle for traditional current transformer but causes non zero output in the Hall sensor in our current transformer resulting a deterioration balance between two mmf's. $R^2$ value determines compatibility between primary current and calculated primary current or estimated primary current.

**Table 1.** Obtained parameters and estimated primary current values

| DC | | | | AC | | | |
|---|---|---|---|---|---|---|---|
| $p_1$ | $p_2$ | $p_3$ | IpE (A) | $p_1$ | $p_2$ | $p_3$ | IpE (A) |
| 0 | 0 | 2 | 0.153 | 0 | 10 | 1 | 0.152 |
| 34.956 | -6.982 | 2.282 | 0.202 | -10.435 | 0.836 | 1.856 | 0.197 |
| 22.480 | -5.635 | 2.251 | 0.255 | 0.011 | -0.356 | 1.886 | 0.250 |
| 11.423 | -4.0594 | 2.202 | 0.304 | -0.982 | -0.210 | 1.881 | 0.300 |
| 6.399 | -3.1642 | 2.167 | 0.351 | -1.380 | -0.138 | 1.878 | 0.349 |
| 5.665 | -3.0068 | 2.160 | 0.401 | -1.262 | -0.163 | 1.879 | 0.399 |
| 4.787 | -2.7866 | 2.148 | 0.452 | -0.990 | -0.231 | 1.883 | 0.448 |
| 3.893 | -2.53 | 2.132 | 0.503 | -0.372 | -0.406 | 1.894 | 0.498 |
| 3.130 | -2.2825 | 2.114 | 0.553 | -0.069 | -0.503 | 1.901 | 0.549 |
| 2.679 | -2.1194 | 2.101 | 0.603 | 0.0381 | -0.541 | 1.904 | 0.598 |
| 2.269 | -1.9557 | 2.087 | 0.653 | 0.184 | -0.598 | 1.909 | 0.649 |
| 1.980 | -1.8289 | 2.075 | 0.703 | 0.247 | -0.625 | 1.911 | 0.698 |
| 1.769 | -1.7284 | 2.065 | 0.754 | 0.316 | -0.657 | 1.914 | 0.749 |
| 1.552 | -1.6171 | 2.052 | 0.804 | 0.335 | -0.667 | 1.915 | 0.800 |
| 1.411 | -1.5391 | 2.043 | 0.855 | 0.317 | -0.657 | 1.914 | 0.849 |
| 1.268 | -1.4543 | 2.032 | 0.905 | 0.342 | -0.671 | 1.916 | 0.899 |
| 1.141 | -1.374 | 2.021 | 0.954 | 0.352 | -0.677 | 1.917 | 0.950 |
| 1.051 | -1.3138 | 2.012 | 1.006 | 0.340 | -0.670 | 1.916 | 0.999 |
| 0.959 | -1.2489 | 2.002 | 1.055 | 0.345 | -0.673 | 1.916 | 1.050 |
| 0.887 | -1.1953 | 1.994 | 1.106 | 0.341 | -0.670 | 1.916 | 1.099 |
| 0.824 | -1.1459 | 1.985 | 1.157 | 0.347 | -0.674 | 1.916 | 1.150 |
| 0.756 | -1.0901 | 1.975 | 1.207 | 0.344 | -0.672 | 1.916 | 1.199 |
| 0.699 | -1.0408 | 1.966 | 1.258 | 0.346 | -0.674 | 1.916 | 1.250 |
| 0.648 | -0.995 | 1.957 | 1.308 | 0.341 | -0.670 | 1.915 | 1.301 |
| 0.602 | -0.9513 | 1.948 | 1.359 | 0.332 | -0.662 | 1.914 | 1.351 |
| 0.559 | -0.9092 | 1.939 | 1.408 | 0.327 | -0.657 | 1.913 | 1.402 |
| 0.523 | -0.8732 | 1.931 | 1.460 | 0.318 | -0.648 | 1.911 | 1.451 |
| 0.488 | -0.8359 | 1.923 | 1.511 | 0.311 | -0.640 | 1.909 | 1.502 |
| 0.453 | -0.7985 | 1.914 | 1.560 | 0.304 | -0.633 | 1.907 | 1.552 |
| 0.424 | -0.7653 | 1.906 | 1.612 | 0.296 | -0.624 | 1.905 | 1.603 |
| 0.395 | -0.7313 | 1.897 | 1.663 | 0.288 | -0.615 | 1.903 | 1.654 |
| 0.367 | -0.6975 | 1.888 | 1.713 | 0.279 | -0.604 | 1.900 | 1.704 |
| 0.340 | -0.6647 | 1.879 | 1.763 | 0.270 | -0.593 | 1.897 | 1.755 |
| 0.318 | -0.6357 | 1.871 | 1.814 | 0.260 | -0.580 | 1.894 | 1.806 |
| 0.296 | -0.6069 | 1.863 | 1.866 | 0.250 | -0.567 | 1.890 | 1.857 |
| 0.274 | -0.5767 | 1.854 | 1.916 | 0.239 | -0.553 | 1.886 | 1.906 |
| 0.254 | -0.5485 | 1.845 | 1.966 | 0.230 | -0.541 | 1.882 | 1.959 |
| 0.235 | -0.5223 | 1.837 | 2.017 | 0.220 | -0.526 | 1.878 | 2.009 |
| 0.217 | -0.4961 | 1.829 | 2.068 | 0.209 | -0.511 | 1.873 | 2.060 |
| 0.201 | -0.4707 | 1.820 | 2.118 | 0.200 | -0.496 | 1.868 | 2.112 |
| 0.185 | -0.4464 | 1.812 | 2.168 | 0.189 | -0.480 | 1.863 | 2.163 |
| 0.171 | -0.4236 | 1.804 | 2.218 | 0.179 | -0.463 | 1.857 | 2.214 |
| 0.158 | -0.4023 | 1.797 | 2.269 | 0.168 | -0.447 | 1.851 | 2.264 |
| 0.145 | -0.3812 | 1.789 | 2.319 | 0.158 | -0.431 | 1.846 | 2.315 |
| 0.134 | -0.3622 | 1.782 | 2.369 | 0.149 | -0.415 | 1.840 | 2.368 |
| 0.123 | -0.3438 | 1.775 | 2.419 | 0.140 | -0.399 | 1.834 | 2.417 |
| 0.113 | -0.3264 | 1.768 | 2.469 | 0.131 | -0.383 | 1.828 | 2.469 |
| 0.105 | -0.3101 | 1.762 | 2.520 | 0.122 | -0.367 | 1.821 | 2.519 |
| 0.096 | -0.294 | 1.755 | 2.569 | 0.113 | -0.351 | 1.815 | 2.570 |
| 0.088 | -0.2795 | 1.749 | 2.618 | 0.105 | -0.336 | 1.809 | 2.619 |
| 0.082 | -0.2664 | 1.744 | 2.668 | 0.098 | -0.322 | 1.803 | 2.669 |
| 0.076 | -0.2545 | 1.738 | 2.716 | 0.091 | -0.309 | 1.797 | 2.719 |
| 0.071 | -0.2444 | 1.734 | 2.765 | 0.086 | -0.297 | 1.792 | 2.768 |
| 0.066 | -0.2351 | 1.730 | 2.814 | 0.080 | -0.286 | 1.787 | 2.816 |
| 0.062 | -0.2271 | 1.726 | 2.862 | 0.076 | -0.277 | 1.783 | 2.864 |
| 0.059 | -0.2207 | 1.723 | 2.909 | 0.072 | -0.269 | 1.780 | 2.911 |
| 0.057 | -0.216 | 1.721 | 2.957 | 0.069 | -0.263 | 1.777 | 2.958 |
| 0.056 | -0.2126 | 1.719 | 3.004 | 0.068 | -0.260 | 1.775 | 3.004 |

$\overline{I_{P_i}}$ to indicate the average value of the primary currents, The mathematical expression of $\overline{I_{P_i}}$ and $R^2$ are [19]

$$\overline{I_{P_i}} = \frac{1}{n}\sum_{i=1}^{n} I_{P_i} \ , \qquad (15)$$

$$R^2 = 1 - \frac{\sum_{i=1}^{n}(I_{P_i} - I_{P_C})^2}{\sum_{i=1}^{n}(\overline{I_{P_i}} - I_{P_C})^2} \ or \ R^2 = 1 - \frac{\sum_{i=1}^{n}(I_{P_i} - I_{P_E})^2}{\sum_{i=1}^{n}(\overline{I_{P_i}} - I_{P_E})^2} . \qquad (16)$$

Before estimation, $R^2$ values for DC and AC measurements are % 96.2739 and % 93.5235 respectively. After estimation $R^2$ values for DC and AC measurements are % 99.9805 and % 99.9884 respectively.

## Conclusions

In this study, a Hall Effect current transformer measuring DC and AC current is designed. A voltage controlled current circuit that will ensure necessary current in a closed loop is established and related measurements are carried out. However, it is seen that errors originate from the Hall sensor, electronic circuit components and other factors. This situation causes deterioration of linearity in measurement results.

With application of the real time parameter estimation, the mathematical model is obtained depending on measurement voltage and the primary current. By using the proposed model, a more linear current measurement can be carried out without using external compensation circuit [23, 24]. Real time observation allows experimenter to examine linearity during the experiment. Compatibility between the reference primary current and measurement voltage increase to % 99.9805 for DC and % 99.9884 for AC measurements.

For further studies, it will be useful to study linearity of the Hall Effect current transformer by means of different analysis methods for theoretical and practical applications.

## Acknowledgements

This study is supported by T.R Marmara University Scientific Research Project Presidency; under project no 2003 FEN-106/020603.

## References

1. **Dzierzanowski W., Miedzinski B., Okraszewski Z.** Directional relay with a Hall sensor for mine MV feeders with no effective earthing // Electronics and Electrical Engineering – Kaunas: Technologija, 2006. – No. 1(65). – P.25–27.
2. **Jankauskas Z.** Currrent Distribution in a Magnetized Solid-State Plasma // Electronics and Electrical Engineering – Kaunas: Technologija, 1999. – No. 3(21). – P.46–48.
3. **Dzierzanowski W., Miedzinski B., Habrych M., Wang X., Xu L. J.** Analysis of a Magnetic Field Distribution in a Hall Sensor Based Protection. // Electronics and Electrical Engineering. – Kaunas: Technologija, 2008. – No. 4(84). – P. 35–28.
4. **Miedzinski B., Dzierzanowski W., Habrych M., Okraszewski Z.** The Influence of Magnetic Shielding on Selectivity of a Hall Sensor based Protection// Electronics

and Electrical Engineering – Kaunas: Technologija, 2009. – No. 3(91). – P. 89–92.
5. **Honeywell Inc.** Hall Effect Sensing and Application // Micro Switch Sensing and Control. – 2002. – Chapter 5. – P.33–41.
6. **Azzoni D., Rüdiger B., Michel F., Harmut G., Hans-Dieter H., Jürgen K., Andreas N., Alfred V.,** Isolated Current and Voltage Transducer Characteristic Applications Calculations // LEM Corporate Communications. – 1999. – P. 20–22.
7. **Amploc Current Sensors.** Engineer's Reference Handbook. – 2002. – P.1–8.
8. **Magnetics Division of Spang & Company**. Magnetics Cores for Hall Effect Devices // Technical Bulletin. – 1997. – Hed-01. – P. 1–6.
9. **Gilbert J., Devey J.,** Linear Hall Effect sensors, Application Information // Application Note. – Allegro Microsystem Inc, 1998. – No. 27702A. – P. 1–12.
10. **Magnetics Division of Spang & Company**. Power Design // Design Application Notes. – 2006. – Section 4. – P. 12–13.
11. **Allegro Microsystem Inc.** 3515 and 3516 Ratiometric Linear Hall-Effect Sensors. // Data Sheet. – 2005. – No. 27501.10B. – P. 1–10.
12. **Gökmen G.** Design and Calibration of Electronic Current Transformer // Phd. Thesis of Applied Science In Electrical Education. – Istanbul: Institute of Pure and Applied Sciences, Marmara University, 2006. – P. 42–80.
13. **National Semiconductor Corporation**. Op-Amp Circuit Collection // Application Note. – 1978. – No. 31. – P. 1–4.
14. **National Semiconductor Corporation**. An Application Guide for Op-Amps // Application Note. – 1969. – No. 20. – P. 1–3.
15. **Burr-Brown Corporation**. INA110 Fast-Settling FET-Input Instrumentation Amplifier // PDS-645E. – 1993. – P. 1–10.
16. **Stitt R., M., Burt B.** Boost Amplifier Output Swing with Simple Modification // Application Bulletin. – Burr-Brown Corporation, 1990. – AB-016. – P. 1–2.
17. **Burr-Brown Corporation**. OPA633 High Speed Buffer Amplifier // PDS-699B. – 1993. – P. 1–9.
18. **Xin A., Hai B., Jiahua S., Yian Y**. The Hall Current Transformer Modeling and Simulation // Proceedings of IEEE International Conference on Power System Technology. – Beijing, 1998. – Vol. 2. – P. 1015–1020.
19. **Kirkup L.** Principles and Applications of Non-Linear Least Squares: An Introduction for Physical Scientists Using Excel's Solver // Department of Applied Physics, Faculty Of Science, University of Technology. – Sydney, 2007. – P. 7–28.
20. **Recktenwald G.** Least Squares Fitting of Data to A Curve // Department of Mechanical Engineering, Portland State University, – 2001. – P. 15–19.
21. http://atlas.cc.itu.edu.tr/~acarh/olcmetek/olcme-d03.pdf, Access date 25.01.2008
22. **Ablameyko S.** Neural Networks for Instrumentation, Measurement and Related Industrial Applications. – IOS Press, 2003. – 290 p
23. **Cristaldi L., Ferrero A., Lazzaroni M., Ottoboni M.** A linearization Method for Commercial Hall-Effect Current Transducers // Instrumentation and Measurement. – IEEE Transactions on Vol. 50, 2001. – Issue 5. – P.1149–1153.
24. **Pereiera J., Postolache O., Girao P.** A Temperature Compensated Power Measurement System Based on a Hall Effect Sensor // IEEE CCECE 2002 Electrical and Computer Engineering Canadian Conference. – 2002. – Vol. 1. – P. 500–503.

Received 2010 01 07

**G. Gokmen, K. Tuncalp. The Design of a Hall Effect Current Transformer and Examination of The Linearity with Real Time Parameter Estimation // Electronics and Electrical Engineering. – Kaunas: Technologija, 2010. – No. 5(101). – P. 3–8.**

Today, the Hall sensor based current measurement is being widely used as they have both AC and DC current measurement capability. The factors such as ratiometric error of Hall sensor, earth or other magnetic effects in sensor location, sensitivity errors originating from temperature or magnetic core, deteriorates measurement linearity. This requires that measurement results are evaluated with mathematical analysis methods. In this study, a closed loop Hall Effect current transformer was designed and its linearity in measurement results is examined by real time parameter estimation based on the least squares method so measurement accuracy was improved and real time observation of linearity error was provided. Ill. 12, bibl. 24, tabl. 1 (in English; abstracts in English, Russian and Lithuanian).

**Г. Гокмен, К. Тунцалп. Исследования трансформатора тока на основе эффекта Холла с учётом моментных изменений параметров // Электроника и электротехника. – Каунас: Технология, 2010. – № 5(101). – C. 3–8.**

Преобразователь Холла широко применяется для измерения постоянного и переменного тока. Исследовано влияние погрешностей, которые создают окружающая температура, механические отклонения, конструкция трансформатора. Для определения погрешностей параметров применен метод наименьших квадратов. Установлены минимальные погрешности на основе теоретических исследований, создан оригинальный трансформатор тока на основе эффекта Холла. Ил. 12, библ. 24, табл. 1 (на английском языке; рефераты на английском, русском и литовском яз.).

**G. Gokmen, K. Tuncalp. Srovės transformatoriaus su Holo efektu projektavimas ir charakteristikų tiesiškumo tyrimas įvertinant momentinius parametrus // Elektronika ir elektrotechnika. – Kaunas: Technologija, 2010. – Nr. 5(101). – P. 3–8.**

Holo jutiklis plačiai taikomas nuolatinei ir kintamajai srovei matuoti. Būtina atkreipti dėmesį į tokius veiksnius, kaip įžeminimą ar magnetinius efektus jutiklio montavimo vietoje, jautrumo paklaidas, atsirandančias dėl temperatūros ar šerdies. Todėl matavimo rezultatams reikia pritaikyti matematinės analizės metodus. Suprojektuotas srovės transformatorius su Holo efektu. Ištirtas charakteristikų tiesiškumas įvertinant realius parametrus. Taikant mažiausiųjų kvadratų metodą, padidėjo matavimo tikslumas. Il. 12, bibl. 24, lent. 1 (anglų kalba; santraukos anglų, rusų ir lietuvių k.).